23rd International Congress of Mechanical Engineering
December 6-11, 2015, Rio de Janeiro, RJ, Brazil

On the Elastodynamics of Parallel Kinematic Machines

Alessandro Cammarata
Rosario Sinatra
Università di Catania, Dipartimento di Ingegneria Industriale, Viale A. Doria 6, 95125, Catania, Italy
acamma@dii.unict.it, rsinatra@dii.unict.it

Abstract. *This paper proposes a methodology based on the Matrix Structural Analysis for the study of the elastodynamics of PKMs. The method can be used to combine rigid and flexible parts through different types of joints that are implicitly included without resorting to the Lagrange multipliers. The flexible bodies must be reduced to two-nodes elastic elements and may be of different nature: Euler or Timoshenko beams, super-elements obtained through FEM, continuous elements. The method is applied to the planar 2-PRRR and to the spatial 3T1R PKM to show some feasible applications in terms of natural frequencies and modes determination.*

Keywords: *elastodynamics, parallel robots, natural frequencies*

1. INTRODUCTION

The elastodynamics of Parallel Kinematic Machines (PKMs) becomes of outmost importance with the increase in performance. The need to reduce the working time and the power required to perform an operation pushes designers to provide a careful analysis of the distribution of mass and stiffness of the parts composing a PKM. At the same time, light materials such as aluminum alloys, carbon fibre or titanium are used to reduce the moving masses without weakening the structural integrity of the robot.

Researchers and companies seek to develop reliable analysis methods and optimization techniques to increase the performances of mechanisms and robots under the elastodynamical point of view. A first classification existing in the literature includes three different approaches: the Finite Element Analysis (FEA), the Matrix Structural Analysis (MSA) and the Virtual Joint Method (VJM).

FEA is still the most-used strategy to analyze the structural behavior of a mechanical system for its reliability and feasibility to model each part of a mechanical system with great detail. The main drawback of FEA is that it implies very tedious and time-consuming routines as FEA models need to be re-meshed over and over again when the robot pose is changed. There is a broad bibliography of FEA but it is beyond the scope of our article.

The MSA introduces some simplifications to FEA that make it more suitable for optimization, considerably reducing the computational time. MSA models operate with large elements like beams, arcs, cables or superelements, (Soares Júnior *et al.*, 2015). In (Huang *et al.*, 2002) the authors use an MSA approach based on superposition principle and virtual work to estimate the stiffness of a Tripod-based PKM. In (Clinton *et al.*, 1997) the stiffness matrix of a Stewart-Gough platform has been derived without considering bending of the links. Other approaches (Deblaise *et al.*, 2006) considered the minimization of the potential energy of a PKM, augmented adding the kinematic constraints by means of the Lagrange multipliers, to find the global stiffness matrix.

While FEA and MSA methods are based on *distributed stiffness* the VJM employs *lumped stiffness*. One of the first application to PKMs comes from the work of Gosselin (Gosselin, 1990) which expanded a rigid-body model of a PKM by adding lumped springs, i.e. “virtual joints”, to take into account the elastic deformations of the actuators. In the approach followed by Gosselin the stiffness matrix of a PKM is mapped onto its workspace by means of its Jacobian matrix.

The problem of studying the vibrations of PKMs is relatively new and extends the stiffness methodology discussed above. It arises primarily from the need to optimize the structure of PKMs inside their workspace. In (Krefft and Hesselbach, 2005) the authors discuss different performance criteria to optimize the inertia/swiftness optimal without affecting the stiffness. The elastodynamics equations are obtained through linearization of the non-linear equations of motion. The stiffness is added in the model using a VJM approach. In (Piras *et al.*, 2005) FEA and Kineto-elastodynamics (KED) are used to find the natural frequencies of a planar PKM with flexible links. Similar approaches have been used in (Zhao *et al.*, 2010; Wu *et al.*, 2013; Song *et al.*, 2015).

In (Rognant *et al.*, 2010) the authors formulate a Lagrangian method for the elastodynamics of PKMs using shape functions based on Hermite polynomials to interpolate the elastic displacements due to bending phenomenon.

In (Briot and Khalil, 2013) the Generalized Newton-Euler model is combined with the principle of virtual powers for the symbolic calculation of the dynamic model of flexible PKMs. The Jacobian matrices defining the kinematic constraints are computed using recursive calculations that decrease the number of operators.

A different approach is proposed in (Portman *et al.*, 2014) in which the authors implement DynCSV: a quadratic form associated with the matrix of the Newton-Euler equations for a platform considered as an unconstrained rigid body on six elastic supports.

In (Cammarata *et al.*, 2013) the authors introduce a general method for the elastodynamics of PKMs based on MSA and implicit joint constraints. The novelty of the method is that the linearized equations of elastodynamics are directly derived without performing the linearization of the nonlinear equations of motions. Besides, joints are naturally included in the method without using the Lagrangian multipliers. All this results in an ease of implementation and a great speed of calculation for optimization problems, as demonstrated in (Cammarata and Sinatra, 2014).

Here we extend the formulation developed by the same authors using a unique case to study the flexible-flexible and flexible-rigid couplings. In Section 2 the elastodynamic model is described along with a mathematical background. The expressions for the generalized stiffness and inertia matrix are analytically derived. In Section 3 the planar 2-$\underline{\text{P}}$RRR and the spatial 3T1R SMG are studied and compared to FEM for validation. Finally, conclusions summarize the content and purpose of the paper.

2. ELASTODYNAMIC MODEL

The proposed method is based on small displacements and Euler angles to describe rotations, while links are modeled by means of matrix structural elements. Here we consider generic two-node beams meaning that Euler or Timoshenko beams can be used. Besides 12×12 numerical stiffness matrices obtained through commercial FE software can be implemented as well.

The following recalls some concepts useful to understand the elastodynamics analysis.

2.1 Small displacements and joint-matrices

A nodal displacement array is a six-dimensional array with three translational followed by three rotational displacements:

$$\mathbf{u} = \begin{bmatrix} u_x & u_y & u_z & u_\varphi & u_\theta & u_\psi \end{bmatrix}^T \tag{1}$$

Joints introduce kinematic constraints between bodies of a mechanism that must be rewritten in terms of constraint equations between adjacent nodes. In particular, considering two nodes, belonging to two consecutive links bonded by a joint, it is possible to express the kinematic constraint provided by the joint through an equation among displacements:

$$\mathbf{u}_1^2 = \mathbf{u}_2^1 + \mathbf{H}\boldsymbol{\theta} \tag{2}$$

in which subscripts of nodal displacements are referred to the link, while superscripts relate to one of the two end-nodes of the link. The joint-matrix $\mathbf{H}$ and the array $\boldsymbol{\theta}$ depend on the joint type: the former containing unit vectors indicating geometric axes, the latter including joint displacements and rotations. Below we write the joint-matrices of some common kinematic pair:

Prismatic joint:

$$\mathbf{h}_P = \begin{bmatrix} \mathbf{e} \\ \mathbf{0} \end{bmatrix}, \quad \theta_P = s \tag{3}$$

where $\mathbf{e}$ is the unit vector along the axis of the prismatic joint P and s is the elongation along the said axis.

Revolute joint:

$$\mathbf{h}_R = \begin{bmatrix} \mathbf{0} \\ \mathbf{e} \end{bmatrix}, \quad \theta_R = \theta \tag{4}$$

where $\mathbf{e}$ is the unit vector along the axis of the revolute joint R and θ is the angle of rotation about the said axis.

Universal joint:

$$\mathbf{H}_U = \begin{bmatrix} \mathbf{0} & \mathbf{0} \\ \mathbf{e}^1 & \mathbf{e}^2 \end{bmatrix}, \quad \boldsymbol{\theta}_U = \begin{bmatrix} \theta^1 \\ \theta^2 \end{bmatrix} \tag{5}$$

where $\mathbf{e}^1$ and $\mathbf{e}^2$ are the unit vectors along the axes of the universal joint U and θ^1 and θ^2 are the angles of rotation about the axes of U.

Spherical joint:

$$\mathbf{H}_S = \begin{bmatrix} \mathbf{0} & \mathbf{0} & \mathbf{0} \\ \mathbf{e}^1 & \mathbf{e}^2 & \mathbf{e}^3 \end{bmatrix}, \quad \boldsymbol{\theta}_S = \begin{bmatrix} \theta^1 \\ \theta^2 \\ \theta^3 \end{bmatrix} \tag{6}$$

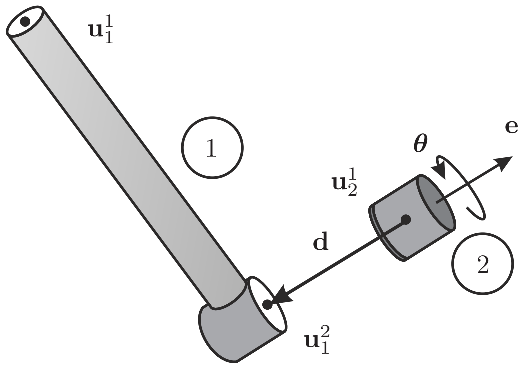

Figure 1. Coupling between two consecutive links.

where $\mathbf{e}^1$, $\mathbf{e}^2$ and $\mathbf{e}^3$ are the unit vectors along the axes of the spherical joint S and θ^1, θ^2 and θ^3 are the angles of rotation about the axes of S.

The described constraint equations are used to consider joints contribute to elastodynamics in a direct way without using Lagrangian multipliers to introduce joint constraints.

2.2 Rigid-body displacement matrix

Let us consider a rigid body and two generic points A and B inside its volume, besides let $\mathbf{d}$ be the vector pointing from A to B. If the body can accomplish only small displacements/rotations, let $\mathbf{p}_A$ be the displacement of point A and $\mathbf{r}$, be the axial vector of the small rotation matrix $\mathbf{R}$. Upon these assumptions, the displacement arrays $\mathbf{u}_A$ and $\mathbf{u}_B$ of A and B, respectively, are tied through the rigid-body displacement matrix $\mathbf{G}_A^B$, i.e.

$$\mathbf{u}_B = \mathbf{G}_A^B \mathbf{u}_A, \quad \mathbf{G}_A^B = \begin{bmatrix} \mathbf{1} & -\mathbf{D} \\ \mathbf{O} & \mathbf{1} \end{bmatrix}, \quad \mathbf{u}_A = \begin{bmatrix} \mathbf{p}_A \\ \mathbf{r} \end{bmatrix}, \quad \mathbf{u}_B = \begin{bmatrix} \mathbf{p}_B \\ \mathbf{r} \end{bmatrix} \tag{7}$$

where $\mathbf{1}$ and $\mathbf{O}$, respectively, are the 3×3 identity- and zero-matrices and $\mathbf{D}$ is the Cross-Product Matrix (C.P.M.) of $\mathbf{d}$, (Angeles, 2007).

2.3 Generalized Stiffness Matrix

Figure 1 describes a flexible body 1 coupled to a second body, either flexible or rigid by means of a joint. Let $\mathbf{u}_i^1$ and $\mathbf{u}_i^2$ denote the displacement arrays of the two end-nodes n_i^1 and n_i^2 of the *i*th-body. Recalling eq.(2), the displacement array $\mathbf{u}_1^2$ can be expressed in terms of $\mathbf{u}_2^1$, belonging to the second body, and $\boldsymbol{\theta}$, i.e.

$$\mathbf{u}_1^2 = \mathbf{G}\mathbf{u}_2^1 + \mathbf{H}\boldsymbol{\theta} \tag{8}$$

in which the matrix $\mathbf{G}$ is derived from the vector $\mathbf{d}$ pointing from n_2^1 towards n_1^2 and is used to introduce a rigid-body displacement. When the nodes n_2^1 and n_1^2 coincide $\mathbf{G}$ becomes the identity matrix $\mathbf{1}_6$. The strain energy V_1 of the flexible body is function of the nodal displacement arrays $\mathbf{u}_2^1$ and $\mathbf{u}_2^2$, i.e.

$$V_1 = \frac{1}{2} \begin{bmatrix} \mathbf{u}_1^1 \\ \mathbf{u}_1^2 \end{bmatrix}^T \begin{bmatrix} \mathbf{K}_1^{1,1} & \mathbf{K}_1^{1,2} \\ \mathbf{K}_1^{2,1} & \mathbf{K}_1^{2,2} \end{bmatrix} \begin{bmatrix} \mathbf{u}_1^1 \\ \mathbf{u}_1^2 \end{bmatrix} \tag{9}$$

with $\mathbf{K}_1$ stiffness matrix of the flexible body 1. By substituting eq.(8) into eq.(9) we find that $V_1 = V_1(\mathbf{u}_1^1, \mathbf{u}_2^1, \boldsymbol{\theta})$. If the joint is passive, its displacement $\boldsymbol{\theta}$ depends on the elastic properties of the system and, therefore, on the two displacements $\mathbf{u}_1^1$ and $\mathbf{u}_2^1$: thus, it implies that V_1 is only function of the two mentioned array, i.e. $V_1 = V_1(\mathbf{u}_1^1, \mathbf{u}_2^1)$. In order to obtain $\boldsymbol{\theta}$ we minimize the strain energy V_1 w.r.t. $\boldsymbol{\theta}$:

$$dV_1/d\boldsymbol{\theta} = \mathbf{0}_6^T \tag{10}$$

where $\mathbf{0}_6$ is the six-dimensional zero array. After rearrangements and simplifications, we find

$$\boldsymbol{\theta} = \mathbf{Y}^1\mathbf{u}_1^1 + \mathbf{Y}^2\mathbf{u}_2^2 \tag{11}$$

where

$$\mathbf{Y}^1 = -(\mathbf{H}^T\mathbf{K}_1^{2,2}\mathbf{H})^{-1}\mathbf{H}^T\mathbf{K}_1^{2,1}, \quad \mathbf{Y}^2 = -(\mathbf{H}^T\mathbf{K}_1^{2,2}\mathbf{H})^{-1}\mathbf{H}^T\mathbf{K}_1^{2,2}\mathbf{G} \tag{12}$$

Then by substituting eq.(11) into eq.(8) and then into eq.(9), we obtain

$$V_1 = \frac{1}{2} \begin{bmatrix} \mathbf{u}_1^1 \\ \mathbf{u}_2^1 \end{bmatrix}^T \begin{bmatrix} \mathbf{K}_{1v}^{1,1} & \mathbf{K}_{1v}^{1,2} \\ \mathbf{K}_{1v}^{2,1} & \mathbf{K}_{1v}^{2,2} \end{bmatrix} \begin{bmatrix} \mathbf{u}_1^1 \\ \mathbf{u}_2^1 \end{bmatrix} \tag{13}$$

where

$$\mathbf{K}_{1v} = \begin{bmatrix} \mathbf{1} & \mathbf{O} \\ \mathbf{X}^1 & \mathbf{X}^2 \end{bmatrix}^T \begin{bmatrix} \mathbf{K}_1^{1,1} & \mathbf{K}_1^{1,2} \\ \mathbf{K}_1^{2,1} & \mathbf{K}_1^{2,2} \end{bmatrix} \begin{bmatrix} \mathbf{1} & \mathbf{O} \\ \mathbf{X}^1 & \mathbf{X}^2 \end{bmatrix} \tag{14}$$

and

$$\mathbf{X}^1 = -\mathbf{H}(\mathbf{H}^T\mathbf{K}_1^{2,2}\mathbf{H})^{-1}\mathbf{H}^T\mathbf{K}_1^{2,1}, \quad \mathbf{X}^2 = \left(\mathbf{1} - \mathbf{H}(\mathbf{H}^T\mathbf{K}_1^{2,2}\mathbf{H})^{-1}\mathbf{H}^T\mathbf{K}_1^{2,2}\right)\mathbf{G} \tag{15}$$

Notice that $\mathbf{K}_{1v}$ is an equivalent stiffness matrix reduced to nodes n_1^1 and n_2^1 that includes implicitly the joint contribute. This aspect is of outmost importance as it avoids the introduction of Lagrangian multipliers to model joints constraints.

For instance, let us consider the case of a revolute joint of unit vector $\mathbf{e}$ in which the two parts composing the revolute pair are not consecutive but far-between of a fixed distance individuated by the vector $\mathbf{d}$. As already outlined the joint-matrix is a six-dimensional array $\mathbf{h}_R = [\mathbf{0}^T\ \mathbf{e}^T]^T$. Then upon substituting the latter into eq.(15), we obtain

$$\mathbf{X}^1 = -\frac{(\mathbf{h}_R\mathbf{h}_R^T)\mathbf{K}_1^{2,1}}{\mathbf{h}_R^T\mathbf{K}_1^{2,2}\mathbf{h}_R}, \quad \mathbf{X}^2 = \left(\mathbf{1} - \frac{(\mathbf{h}_R\mathbf{h}_R^T)\mathbf{K}_1^{2,2}}{\mathbf{h}_R^T\mathbf{K}_1^{2,2}\mathbf{h}_R}\right)\mathbf{G} \tag{16}$$

The expression of $\mathbf{K}_{1v}$ can be derived by means of eq.(14). Similar expressions can be found for the other types of joints.

2.4 Generalized inertia matrix

In this section we describe how to include the inertial properties of links and rigid bodies into the model. The two cases of *lumped* and *consistent* mass, commonly used in the literature, will be discussed separately.

2.4.1 Lumped mass

Mass and inertia are lumped into a unique independent node located at the center of mass of a rigid body. Let m_i and $\mathbf{J}_i$, respectively, be the mass and the inertia matrix of a rigid body, then the generic 6×6 inertia dyad $\widetilde{\mathbf{M}}_i$ can be written as

$$\widetilde{\mathbf{M}}_i = \begin{bmatrix} m_i\mathbf{1} & \mathbf{O} \\ \mathbf{O} & \mathbf{J}_i \end{bmatrix} \tag{17}$$

2.4.2 Consistent mass

Consistent mass approach considers the true distribution of mass inside a flexible body (Shabana, 2012). Let $\mathbf{M}_i$ be the 12×12 matrix associated to the kinetic energy T_i of a beam, where T_i is a quadratic forms into the time-derivatives $\dot{\mathbf{u}}_i^1$, $\dot{\mathbf{u}}_i^2$ of the nodal displacement arrays $\mathbf{u}_i^1$ and $\mathbf{u}_i^2$:

$$T_i = \frac{1}{2}\begin{bmatrix} \dot{\mathbf{u}}_i^1 \\ \dot{\mathbf{u}}_i^2 \end{bmatrix}^T \begin{bmatrix} \mathbf{M}_i^{1,1} & \mathbf{M}_i^{1,2} \\ \mathbf{M}_i^{2,1} & \mathbf{M}_i^{2,2} \end{bmatrix} \begin{bmatrix} \dot{\mathbf{u}}_i^1 \\ \dot{\mathbf{u}}_i^2 \end{bmatrix} \tag{18}$$

Then, it is possible to find how the time-derivative of dependent nodal displacement arrays can be expressed in terms of the time-derivative of the independent ones simply time-differentiating eq.(8). As already obtained for stiffness matrices, it is possible to find a generalized inertia matrix $\mathbf{M}_{1v}$, defined as

$$\mathbf{M}_{1v} = \begin{bmatrix} \mathbf{1} & \mathbf{O} \\ \mathbf{X}^1 & \mathbf{X}^2 \end{bmatrix}^T \begin{bmatrix} \mathbf{M}_1^{1,1} & \mathbf{M}_1^{1,2} \\ \mathbf{M}_1^{2,1} & \mathbf{M}_1^{2,2} \end{bmatrix} \begin{bmatrix} \mathbf{1} & \mathbf{O} \\ \mathbf{X}^1 & \mathbf{X}^2 \end{bmatrix} \tag{19}$$

with $\mathbf{X}^1$ and $\mathbf{X}^2$ previously defined in eq.(16).

2.5 Elastodynamic Equations

The stiffness and inertia matrices are used to describe the coupling of links (platforms) by means of joints. Going from the base platform (BP) to the moving platform (MP) it is possible to assemble the generalized matrices of each leg. The latter can be arranged with common methods coming from FEA to find the global matrices $\mathbf{K}_t$ and $\mathbf{M}_t$ of the PKM. Finally, the linearized elastodynamics equations are readily written as

$$\mathbf{M}_t\ddot{\mathbf{q}} + \mathbf{K}_t\mathbf{q} = \mathbf{0} \tag{20}$$

where $\mathbf{q}$ is the array containing all the displacements of the nodes.

3. CASE STUDY

Here we present two applications of the elastodynamic method to two PKMs: the planar 2-PRRR and the spatial 3T1R Schönflies motion generator (SMG).

3.1 Planar 2-PRRR

The first case study is the planar 2-PRRR PKM, shown in Fig. 2. Two links per leg of type PRRR join the MP to the BP. The actuation of the system is performed by the two prismatic joints.

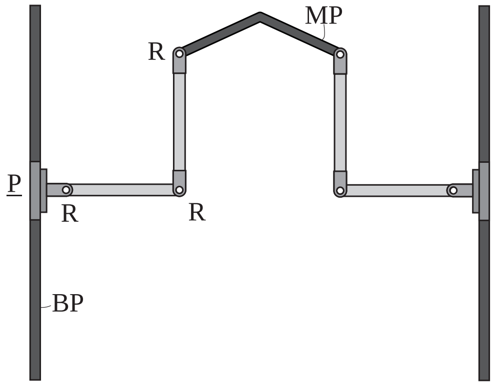

Figure 2. Schematic model of the 2-PRRR manipulator

All links are modeled as straight Euler beams, while MP is modeled as a rigid body. In Table. 1 the geometrical, structural and inertial parameters are reported while Table. 2 reports the first six natural frequencies obtained locking the actuators at the posture of Fig. 2 in which there is no rotation of the MP. The results of the algorithm have been compared to Nastran© for validation. As it can be observed the relative error is very low and the algorithm maintains this robustness even for high frequencies. We found that the first thirty frequencies remain below one percent.

Table 1. The 2-PRRR geometric, inertial and structural parameters

Parameters of the 2-PRRR			
Notation	Description	Value	Unit
L_1	proximal link's length	1	[m]
L_2	distal link's length	1	[m]
d	side length of the MP	$\sqrt{0.5}$	[m]
r	radius of cylindrical links	0.03	[m]
A	link's cross section area	2.827E-03	[m^2]
I	moment of inertia	6.362E-07	[kg m^2]
J	polar moment of inertia	1.272E-06	[kg m^2]
E	Young modulus	210E+09	[Pa]
G	shear modulus	79.545E+09	[Pa]
ρ	density	4222.71	[kg/m^3]
m_p	MP's mass	100	[kg]
$\mathbf{I}_p$	MP's inertia matrix	$0.01 * \mathbf{1}$	[kg m^2]

Table 2. Natural frequencies of the 2-PRRR; *A* indicates the outputs of the algorithm; *B* the outputs of Nastran©

No.	A (Hz)	B (Hz)	rel.-err. [%]
1	3.84E+01	3.84E+01	0.155
2	4.63E+01	4.62E+01	0.192
3	8.19E+01	8.18E+01	0.066
4	1.05E+02	1.05E+02	0.139
5	1.16E+02	1.16E+02	0.397
6	1.18E+02	1.18E+02	0.397

3.2 Spatial 3T1R SMG

Here we apply the method to a complex PKM, the 3T1R SMG, with 4-dof whose kinematics has been studied in (Salgado *et al.*, 2008). Due to the particular kind of constraints generated by the limbs, the MP can accomplish three translations and a rotation around the vertical axis: this motion is referred to as Schönflies motion generator (SMG) and it is typical of SCARA robots largely used in industry for pick-and-place applications. One of the four leg is shown in Fig. 3. It is composed of a distal link connected to the base frame by means of an actuated revolute joint and to a parallelogram linkage, i.e. a Π-joint, by means of a revolute joint. The parallelogram, in turn, is linked to a proximal link by another revolute. Finally, the proximal link is coupled to the MP by a vertical axis revolute joint.

The numerical results have been compared to FEA model for validation. The latter considers solid links while joints have finite burdens and provide their function by means of the coupling of surfaces and screws.

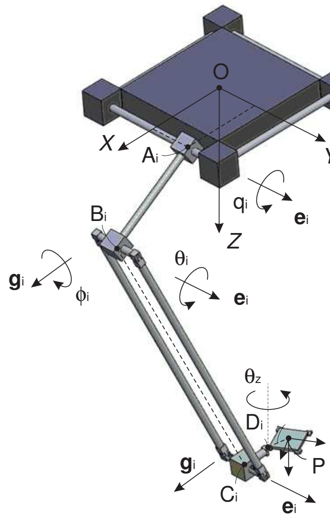

Figure 3. Generic leg of the 3T1R PKM.

In Table 3 the first ten natural frequency of the robot, at the *home pose*, i.e. that with no rotation of the MP, are reported. Results show good agreement with FEA; some discrepancies still occur as all bodies are simulated as flexible to avoid asymmetric contacts between rigid and flexible solids leading to convergence mistakes. In turn, we used a stiffer material to approximate rigid behavior of the MP and rigid links. Finally, Fig. 4 reports the first mode of vibration compared to Ansys© results. As can be observed the first mode shape is determined by the in-plane bending of the Π-joints that yields a twist of the MP around the vertical axis. Notice that even in this case the actuated revolute joints of the BP are locked to prevent rigid motions.

Table 3. The first ten natural frequencies of the 3T1R PKM at the home pose.

Freq.	Algorithm [Hz]	FEM [Hz]	err
1	2.920	3.019	3.28%
2	7.062	7.204	1.97%
3	11.275	11.487	1.85%
4	20.834	21.554	3.34%
5	25.480	25.722	0.94%
6	25.545	25.804	1.00%
7	26.028	26.181	0.58%
8	28.306	28.830	1.82%
9	30.368	31.295	2.96%
10	31.060	32.286	3.80%

4. CONCLUSIONS

A novel model for the elastodynamics analysis of Parallel Kinematic Machines has been proposed. It extends the Matrix Structural Analysis introducing the constraints of the joints in an implicit form. The couplings of a flexible body to another flexible body or to a rigid body have been studied to find the generalized stiffness and inertia matrices. Feasible

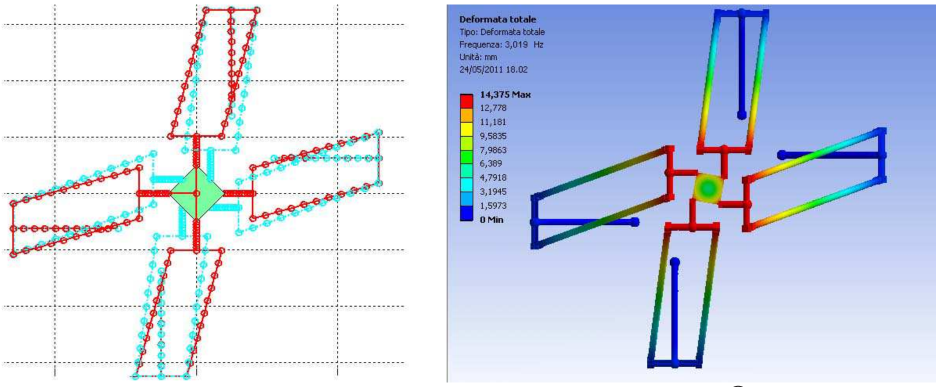

Figure 4. First mode of vibration: Algorithm $vs.$ Ansys©.

applications pertain to the determination of the natural frequencies and modes of vibration inside the workspace, hence two examples have been provided to demonstrate the correctness of the proposed elastodynamic model. The numerical results revealed in good accordance to commercial software results.

5. REFERENCES

Angeles, J., 2007. *Fundamentals of Robotic Mechanical Systems: Theory, Methods and Algorithms, Third edition*, Vol. 3. Springer.

Briot, S. and Khalil, W., 2013. "Recursive and symbolic calculation of the elastodynamic model of flexible parallel robots". *The International Journal of Robotics Research*, p. 0278364913507006.

Cammarata, A., Condorelli, D. and Sinatra, R., 2013. "An algorithm to study the elastodynamics of parallel kinematic machines with lower kinematic pairs". *Journal of Mechanisms and Robotics*, Vol. 5, No. 1, p. 011004.

Cammarata, A. and Sinatra, R., 2014. "Elastodynamic optimization of a 3t1r parallel manipulator". *Mechanism and Machine Theory*, Vol. 73, pp. 184–196.

Clinton, C.M., Zhang, G. and Wavering, A.J., 1997. "Stiffness modeling of a stewart platform based milling machine".

Deblaise, D., Hernot, X. and Maurine, P., 2006. "A systematic analytical method for pkm stiffness matrix calculation". pp. 4213–4219.

Gosselin, C., 1990. "Stiffness mapping for parallel manipulators". *Robotics and Automation, IEEE Transactions on*, Vol. 6, No. 3, pp. 377–382.

Huang, T., Zhao, X. and Whitehouse, D.J., 2002. "Stiffness estimation of a tripod-based parallel kinematic machine". *Robotics and Automation, IEEE Transactions on*, Vol. 18, No. 1, pp. 50–58.

Krefft, M. and Hesselbach, J., 2005. "Elastodynamic optimization of parallel kinematics". pp. 357–362.

Piras, G., Cleghorn, W. and Mills, J., 2005. "Dynamic finite-element analysis of a planar high-speed, high-precision parallel manipulator with flexible links". *Mechanism and Machine Theory*, Vol. 40, No. 7, pp. 849–862.

Portman, V., Chapsky, V. and Shneor, Y., 2014. "Evaluation and optimization of dynamic stiffness values of the pkms: Collinear stiffness value approach". *Mechanism and Machine Theory*, Vol. 74, pp. 216–244.

Rognant, M., Courteille, E. and Maurine, P., 2010. "A systematic procedure for the elastodynamic modeling and identification of robot manipulators". *IEEE Transactions on Robotics*, Vol. 26, No. 6, pp. 1085–1093.

Salgado, O., Altuzarra, O., Petuya, V. and Hernández, A., 2008. "Synthesis and design of a novel 3t1r fully-parallel manipulator". *Journal of Mechanical Design*, Vol. 130, No. 4, p. 042305.

Shabana, A.A., 2012. *Theory of vibration: Volume II: discrete and continuous systems*. Springer Science & Business Media.

Soares Júnior, G., Carvalho, J. and Gonçalves, R., 2015. "Stiffness analysis of multibody systems using matrix structural analysis–msa". *Robotica*, pp. 1–18.

Song, Y., Dong, G., Sun, T. and Lian, B., 2015. "Elasto-dynamic analysis of a novel 2-dof rotational parallel mechanism with an articulated travelling platform". *Meccanica*, pp. 1–11.

Wu, J., Li, T., Wang, J. and Wang, L., 2013. "Stiffness and natural frequency of a 3-dof parallel manipulator with consideration of additional leg candidates". *Robotics and Autonomous Systems*, Vol. 61, No. 8, pp. 868–875.

Zhao, Y., Gao, F., Dong, X. and Zhao, X., 2010. "Elastodynamic characteristics comparison of the 8-pss redundant parallel manipulator and its non-redundant counterpart the 6-pss parallel manipulator". *Mechanism and Machine Theory*, Vol. 45, No. 2, pp. 291–303.

6. RESPONSIBILITY NOTICE

The authors are the only responsible for the printed material included in this paper.